Front. Phys., 2011, 6(2): 151–161
DOI 10.1007/s11467-011-0175-2

REVIEW ARTICLE

Progress in improving thermodynamics and kinetics of new hydrogen storage materials

Li-fang SONG (宋莉芳)[1,2], **Chun-hong JIANG** (姜春红)[1,2], **Shu-sheng LIU** (刘淑生)[1,2], **Cheng-li JIAO** (焦成丽)[1,2], **Xiao-liang SI** (司晓亮)[1,2], **Shuang WANG** (王爽)[1,2], **Fen LI** (李芬)[1], **Jian ZHANG** (张箭)[1], **Li-xian SUN** (孙立贤)[1,†], **Fen XU** (徐芬)[1,3,*], **Feng-lei HUANG** (黄凤雷)[4]

[1] *Materials and Thermochemistry Laboratory, Dalian Institute of Chemical Physics, Chinese Academy of Sciences, Dalian 116023, China*

[2] *Graduate School of the Chinese Academy of Sciences, Beijing 100049, China*

[3] *Faculty of Chemistry and Chemical Engineering, Liaoning Normal University, Dalian 116029, China*

[4] *Beijing Institute of Technology, State Key Laboratory of Explosion Science & Technology, Beijing 100081, China*

E-mail: †*lxsun@dicp.ac.cn*, **xufen@lnnu.edu.cn*

Received October 28, 2010; accepted January 26, 2011

Hydrogen storage material has been much developed recently because of its potential for proton exchange membrane (PEM) fuel cell applications. A successful solid-state reversible storage material should meet the requirements of high storage capacity, suitable thermodynamic properties, and fast adsorption and desorption kinetics. Complex hydrides, including boron hydride and alanate, ammonia borane, metal organic frameworks (MOFs), covalent organic frameworks (COFs) and zeolitic imidazolate frameworks (ZIFs), are remarkable hydrogen storage materials because of their advantages of high energy density and safety. This feature article focuses mainly on the thermodynamics and kinetics of these hydrogen storage materials in the past few years.

Keywords ammonia borane, hydrogen storage materials, hydrides, kinetics, metal organic frameworks, thermodynamics

PACS numbers 88.30.R-, 82.20.-w, 82.60.-s, 89.75.-k, 62.23.St, 68.43.Mn

Contents

1 Introduction

Hydrogen is an ideal energy carrier which holds tremendous promise as a new renewable and clean energy option because it is light, highly abundant and its oxidation product, water, is environmentally friendly. On the other hand, hydrogen is flammable, particularly explosive, highly diffusive, and its volume density is only one three thousandth of that of gasoline. Therefore, hydrogen storage concerns both hydrogen production and hydrogen application, and assumes a critical role in initiating a hydrogen economy. The ultimate goal related to hydrogen storage is to develop technologies with high energy density, high efficiency and safety [1–3]. Up to now, there are three ways to consider in hydrogen storage:

high pressure gas, low temperature liquid and solid-state hydrogen storage materials. Hydrogen storage under high gaseous pressure has been applied with some success but the drawback in this solution is the unresolved safety problem, which makes the solution totally incompatible for large-scale private vehicles. Liquid hydrogen storage at low temperature has a higher volume density, but the energy waste resulting from hydrogen liquefaction can reach up to 50% of the storage. Moreover, liquid hydrogen is readily volatile and still stays significantly unsafe. Hydrogen storage involving chemical reactions or physical adsorption in some solid materials provides devices with high energy density and safety is no longer a problem: it is undeniably the most promising way for hydrogen storage [4]. Great efforts have been made to develop materials that can hold sufficient hydrogen and possess suitable thermodynamic and kinetic properties. The key point is to prepare materials with high capacity that can absorb/desorb hydrogen reversibly. Various hydrogen storage systems, such as metal hydrides, chemical hydrides, complex hydrides, and metal organic frameworks have attracted increasing interest and been explored for onboard hydrogen storage applications [5]. Among the various hydrogen storage systems, thermodynamics and kinetics of complex hydride and metal organic frameworks are discussed in the present paper.

2 Complex hydrides

Compared with traditional metal hydrides (e.g. LiH, $LaNi_5H_6$), complex metal hydrides have recently got much attention as a promising new kind of hydrogen storage material because of their high hydrogen storage capacity and moderate operation temperature. However, the intensive investigation of complex hydrides did not begin until Bogdanović *et al.* reported the reversible hydrogen storage of Ti-doped $NaAlH_4$ in 1997 [6]. Light weight complex hydrides, namely alanates, borohydrides and amides, are mostly attractive candidates for hydrogen storage. They have the similar formula, $M_m(XH_x)_n$ (M=Li, Na, K, Mg, Ca, etc.; X=Al, B, N). Among them, $NaAlH_4$ has been studied roundly, but its capacity is only 5.6 wt% for practical use. Herein, we will focus on some new materials with higher capacities, like $LiAlH_4$, $LiBH_4$ and $LiNH_2$.

2.1 $LiAlH_4$

$LiAlH_4$ releases 7.9 wt% H_2 below 220°C, corresponding to the first two steps [Eq. (1) and Eq. (2)] of decomposition [7, 8]. Apparently, the temperature is still high considering the U. S. Department of Energy (DOE) target of 80°C. In addition, the reversibility of $LiAlH_4$ is poor. Therefore, many efforts have been done to overcome these disadvantages, such as mechanical milling, doping catalysts, combination with other hydrides and solvent coordination. The corresponding thermodynamics and kinetics investigations after these treatments are essential to the understanding of their influence on $LiAlH_4$ and, further, on improvement of the hydrogen storage properties of $LiAlH_4$.

$$3\ LiAlH_4 \xrightarrow{150-175^{\circ}C} Li_3AlH_6 + 2\ Al + 3\ H_2,\quad 5.3\ wt\%\ H_2 \tag{1}$$

$$Li_3AlH_6 \xrightarrow{180-220^{\circ}C} 3\ LiH + Al + 3/2\ H_2,\quad 2.6\ wt\%\ H_2 \tag{2}$$

2.1.1 *Mechanical milling*

Mechanical milling can decrease the starting temperature of reactions (1) and (2) to some extent, depending on the milling conditions and material supplier. Ares *et al.* [9] reported that 30 min milling reduces the crystallite size of $LiAlH_4$ to about 90 nm from the original 300 nm. Hence, the diffusion distance is reduced. The activation energy is lowered and the kinetics is improved for the first step [Eq. (1)] of $LiAlH_4$ decomposition. But for the second step [Eq. (2)], there exist different results from the influence of milling on the kinetics [9–11]. On the other hand, mechanical milling can hardly change the thermodynamics of $LiAlH_4$. Too long time milling can lead to the partial decomposition of $LiAlH_4$. So mechanical milling alone has limited influence on $LiAlH_4$, and it is usually used as a common method of doping catalysts and combination with other hydrides.

2.1.2 *Doping catalysts*

Various catalysts have been used on $LiAlH_4$ and could be classified into five categories: pure metals, such as Ti [12–15], Ni [15, 16], and V [15]; alloys, like $TiAl_3$[12, 14], Ti_3Al [14]; metal halides, such as TiF_3 [8, 17], $TiCl_4$ [12, 18], $TiCl_3$ [19], VCl_3 [20, 21], $LaCl_3$ [16], $ZrCl_4$ [22], $HfCl_4$ [22], $TiCl_3 \cdot \frac{1}{3}AlCl_3$ [13], VBr_3 [21] and $NiCl_2$ [23]; carbon materials, such as CNFs (carbon nanofibers) and Vulcan XC72R [15, 24]; composites, like VCl_3@CNFs [24]. These catalysts reduce the decomposition temperature of $LiAlH_4$ more or less and improve the kinetics of dehydrogenation. Among them, metal halides perform best. Doping with 2 mol% $TiCl_3 \cdot \frac{1}{3}AlCl_3$ [13] or 4 mol% $HfCl_4$ [22] makes $LiAlH_4$ decompose around 100°C. Moreover, under the catalytic effect of 4 mol% TiF_3 [8], $LiAlH_4$ starts to decompose at 60°C and releases 5.0 wt% H_2 at up to 145°C. A thermodynamic change of Li_3AlH_6 was reported by Chen *et al.* [13] when $TiCl_3 \cdot \frac{1}{3}AlCl_3$ was doped into $LiAlH_4$, resulting in the partial reversibility.

2.1.3 Combination with other hydrides

Different hydrides combined with $LiAlH_4$ may form new compounds or just mixtures. Under mechanical milling, LiH and NaH can react with $LiAlH_4$ to form Li_3AlH_6 [25] and Na_2LiAlH_6 [26], respectively. The occurrence of these reactions indicates that Li_3AlH_6 and Na_2LiAlH_6 are more stable than $LiAlH_4$, which is also proved by the increase of their dissociation enthalpy [25, 26]. Although their dehydrogenation temperatures increase to some extent, the reversibility is greatly improved as compared with $LiAlH_4$.

Most hydrides form mixtures rather than react with $LiAlH_4$ under milling. Then many multiplex systems have been developed, such as $LiAlH_4$–MgH_2 [27, 28], $LiAlH_4$–CaH_2 [29], $LiAlH_4$–$LiBH_4$ [30] and $LiAlH_4$–$NaBH_4$ [31]. The dehydrogenation of $LiAlH_4$ occurs at lower temperatures and its kinetics has been improved in all the mixtures. But its thermodynamics seems unchangeable. $LiAlH_4$ provides its Al element to combine with Mg and B to form alloys, and it becomes impossible to regain $LiAlH_4$ or Li_3AlH_6 under moderate condition of gas-state hydrogen storage.

2.1.4 Solvent coordination

Wang *et al.* [32] discovered a five-step physiochemical pathway for the rehydrogenation of $LiAlH_4$ from Li_3AlH_6, LiH and Al, and the reactions are shown in Eq. (3):

$$\frac{1}{3}Li_3AlH_6 + \frac{2}{3}Al + H_2 + 4THF \xrightarrow[\text{Ball milling in THF}]{TiCl_3,\ 97.5\ \text{bar}\ H_2} LiAlH_4 \cdot 4THF \xrightarrow[\text{Vacuum}]{60^\circ C} LiAlH_4 + 4THF \quad (3)$$

THF is strongly attached to Li^+ in $LiAlH_4$ and form the four coordinated lithium solvate, hence the enthalpy changes and makes it thermodynamically favorable to form $LiAlH_4$·4THF. Graetz *et al.* [33] used active Al and easily got $LiAlH_4$·4THF after stirring the THF slurry of LiH and Al under 13 bar H_2. The desorption of solvent becomes easier when the solvent is changed to Me_2O because of the thermodynamic unstability of Li–Me_2O bond compared with Li–THF bond [34]. Much work is needed to lower the H_2 pressure and increase the conversion. The solvent coordination method pushes the study of $LiAlH_4$ as a hydrogen storage material and provides an efficient method for other materials.

2.2 $LiBH_4$

$LiBH_4$ releases as high as 13.8 wt% H_2 at a temperature of over 400°C, shown in Eq. (4), and attracts more attention than $LiAlH_4$. But it is only partially restored even at a rigorous condition of 600°C and 35 MPa hydrogen [35]. To lower the operation temperature and improve the kinetics and reversibility of $LiBH_4$, the methods including mechanical milling, doping catalysts and combination with other hydrides have also been applied. Herein, we will not expand these methods.

$$LiBH_4 \rightarrow LiH + B + \frac{3}{2}H_2 \quad (4)$$

The inevitable particle agglomeration and growth lead to the hydrogen storage property degradation. Additionally, it is difficult to obtain freestanding nanopaticles for most hydrides. These obstacles push scientists to seek new methods, like nanoconfinement, which is generally realized by introducing the hydrides into the nanoporous of porous materials through solution impregnation or melt infiltration.

The solution impregnation method is easy to control and used mostly. Fang *et al.* [36] prepared $LiBH_4$/AC (activated carbon) sample, which starts to release hydrogen from 220°C. It is 150°C lower than the onset dehydrogenation temperature of bulk $LiBH_4$. And the kinetics increases one order of magnitude. The rehydrogenation property is greatly improved and more than 6.6 wt% H_2 can be recovered. These improvements are not limited to kinetics, but are extended to thermodynamic change, which can be implied from the increase of the dissociation pressure. Brun *et al.* [37] used carbon monoliths with 0.5 nm pores as the host material and got similar results.

Gross *et al.* [38] applied melt infiltration method to the preparation of nanoconfined $LiBH_4$ with carbon materials with different pore sizes. The corresponding properties are summarized in Table 1. It is clear that nanoconfinement greatly enhances the properties of hydrogen storage, and smaller pores are inclined to obtain better kinetics and higher reversibility. SBA–15 is also used as an excellent porous material in confining $LiBH_4$, whose onset dehydrogenation temperature is reduced to 150°C. But $LiBH_4$/SBA–15 shows poor reversibility due to the formation of Li_2SiO_3 and Li_4SiO_4 [39].

Table 1 The hydrogen storage properties of $LiBH_4$ incorporated into carbon scaffolds. (after Ref. [38])

Host material	Carbon	Aerogel	Graphite
Pore size /nm	13	25	Nonporous
Loading amount /wt%	25–30	45–50	–
Onset temperature of dehydrogenation /°C[a]	260	260	380
Hydrogen desorbed up to 600°C /wt%	4.6	6.4	3.6
Hydrogen resorbed ratio /%	63	48	36
Activation energy /(kJ·mol^{-1})	103	111	146
Dehydrogenation rate at 300°C /(wt% ·h^{-1})	12.5	7.8	0.22

[a]The data are evaluated from the TGA curves in Ref. [38].

2.3 Li–N–H system

In 1910, Dafert and Miklauz reported that when Li_3N reacted with H_2, Li_3NH_4 was formed [40]. In fact, Li_3NH_4 is the mixture of $LiNH_2$ and 2LiH. Because lithium amide will decompose to lithium imide and ammonia at increased temperature [41], no investigation on the reverse reaction was done. In 2002, the hydrogenation of Li_3N and the dehydrogenation of the hydrogenated Li_3N were studied, which can be used as a new hydrogen storage material [42]. A large amount of hydrogen (10.4 wt%) were reversibly stored in Li_3N by the following two-step reactions:

$$Li_3N+2H_2 \leftrightarrow Li_2NH+LiH+H_2 \leftrightarrow LiNH_2+2LiH \quad (5)$$

However, the standard enthalpy change of the first reaction in Eq. (5) could be calculated to be –148 kJ·mol^{-1} H_2 from each standard enthalpy of formation. The large magnitude requires a very high temperature over 430°C for complete recovery of Li_3N from the hydrogenated state. While the second reaction has a much smaller enthalpy change calculated to be –44.5 kJ·mol^{-1} H_2 and still a large amount of hydrogen storage capacity of 6.5 wt% [43]. Therefore, the latter reaction [Eq. (6)] is still considered to be suitable for hydrogen storage and has been investigated extensively [43–50]:

$$LiNH_2 + LiH \leftrightarrow Li_2NH + H_2 \quad (6)$$

2.3.1 Effects of ball milling on ($LiNH_2$ + LiH) system

Mechanical activation via high-energy ball milling is one way to improve the kinetics of the system. The mechanisms are the particle size refinement through ball milling and the introduction of internal defects.

Varin *et al.* [51] studied the effects of ball milling time and different molar ratios (1:1, 1:1.2, 1:1.4) of the mixtures of $LiNH_2$ and LiH on hydrogen storage. During a high-energy ball milling of the 1:1 molar ratio mixture, the grain size decreases with increasing milling time, while the specific surface area (SSA) of powder increases up to 25 h milling and then decreases after milling for 100 h, due to the excessive agglomeration of powder particles (Table 2). The activation energy for hydrogen desorption decreases with increasing SSA of powder, and the lowest activation energy is observed for the molar ratio of $LiNH_2$:1.2LiH.

The ball milling process causes excessive heat and lithium amide exceeds its melting temperature at the collision site. To combat the effect of the temperature rise at the collision site, Osborn *et al.* performed the ball milling at 20°C, –40°C, and –196°C with dry ice chilled ethanol and liquid nitrogen as coolants [52, 53]. The powder at –196°C exhibited a stable and significant increase in the hydrogen desorption kinetics, and both crystallite size from XRD and equivalent particle size from SSA are larger for the sample milled at –196°C. NMR analysis indicates that what to blame for the increased kinetics of the milled samples at low temperature is the retention of large amounts of lattice and surface defects that results in an increased diffusion rate, while which are annealed at the collision site at higher milling temperatures.

Table 2 Summary of the calculations of the activation energy of reaction [Eq. (6)]. (after Ref. [51])

Milling time /h	Molar ratio ($LiNH_2$:LiH)	BET specific surface area /($m^2 \cdot g^{-1}$)	Activation energy /(kJ·mol^{-1})
0	1:1	16.5	237.5
1	1:1	26.4	94.9
5	1:1	56.0	89.5
25	1:1	59.6	84.5
25	1:1.2	NA	57.5
25	1:1.4	NA	70.6
100	1:1	45.6	88.0

2.3.2 Partial substitution of Li by Mg

In spite of high storage capacity, Li–N–H system possesses unfavorable thermodynamics [54–56]. Several studies reveal that the replacement of Li by Mg (or $LiNH_2/MgH_2$ mixture) gives rise to a system having favorable combination of thermodynamics, reversible capacity and operating conditions [57–63]. The reversible de/rehydrogenation reactions of this system can be described as:

$$2LiNH_2 + MgH_2 \rightarrow Li_2MgN_2H_2 + 2H_2 \leftrightarrow Mg(NH_2)_2 + 2LiH \quad (7)$$

Dolci *et al.* investigated the hydrogen sorption with different ratios of $Mg(NH_2)_2$/LiH mixtures (1:2, 3:8, 1:4) by in-situ neutron diffraction [64]. Intermediate reaction steps are observed in both absorption and desorption. The thermodynamic properties of the system at 200°C are not changed by increasing the lithium hydride content of the system. Chen *et al.* studied the lowest total energy crystal structure of $Li_2MgN_2H_2$ [65] and the activation energies of the Li–Mg–N–H system with doped TiF_3 by the first principle calculation [66]. The properties of the TiF_3 doped Li–Mg–N–H system had a slight improvement in kinetics of desorption and elucidated a considerable modification in kinetics of rehydrogenation. Wang *et al.* studied the kinetics of hydrogen desorption of the $Mg(NH_2)_2$/LiH mixture by measuring desorption rates at various temperatures [67], and suggested the methods of exploring suitable dopants to create more vacancies in the matrix and activating the N–H with an electromagnetic field to improve the desorption kinetics. Then Ma *et al.* introduced two transition metal nitrides TaN and TiN as catalysts for the Li–Mg–N–

H system [68], both nitrides are catalytically active for accelerating the dehydrogenation reaction and the catalytic enhancement well persists without hydrogen capacity loss. V, V_2O_5 and VCl_3 catalysts were admixed with $Mg(NH_2)_2$/LiH mixture [59], and all these catalysts lead to the reduction in the decomposition temperature and the corresponding enhancement in the desorption kinetics. The optimum catalyst is VCl_3, and the decomposition temperature changes from 80°C to 50°C. Also, the desorption kinetics is enhanced up to 38%.

2.3.3 Other composition substitution and catalytic modification

To improve the thermodynamic properties of Li–N–H system, many other new class of complex systems besides Li–Mg–N–H are developed [69–76].

Hydrogen desorption properties of different ratios of $LiNH_2/LiBH_4/MgH_2$ composites (2:1:2, 1:1:1, 2:0.5:1, 2:1:1, 3:1:1.5) were studied by the examination of the effects of reactant stoichiometry [77]. The composites were found to release hydrogen via a complex multistep reaction cascade, which seeded the products of a subsequent reversible hydrogen storage reaction. This so-called autocatalytic reaction sequence was found to generate favorable kinetics, ammonia attenuation, and partial low–temperature reversibility. The optimal ratio (3:1:1.5) releases a total of 9.1 wt% hydrogen. Srinivasan *et al.* prepared $LiNH_2/LiBH_4/MgH_2$ composites with a 2:1:1 molar ratio but with varying milling duration [78]. It is found that the samples with MgH_2 crystallite sizes of approximately 10 nm exhibit lower initial hydrogen release at a temperature of 150°C, and the crystallite size of Li–B–N–H has a significant effect on the amount of hydrogen release with an optimum size of 28 nm.

Pan *et al.* systematically investigated the hydrogen storage properties and mechanisms of a novel Li–Al–N–H system [79]. The Li_3N–AlN mixture milled for 12 h can absorb 5.2 wt% hydrogen with the formation of $LiNH_2$/LiH/AlN, and the dehydrogenation of the hydrogenated sample proceeds with a two step reaction. The presence of AlN in the $LiNH_2$/LiH system significantly improves its dehydrogenation kinetics with a 50°C reduction in the end temperature. Nahm *et al.* illustrated the dehydrogenation properties of combined $LiAlH_4/LiNH_2$ (2:1) mixture and $LiAlH_4$ wet doped with different transition metals (Sc, Ti, and V) in their chloride forms [80]. The $LiAlH_4/LiNH_2$ mixture showed high hydrogen desorption with 7.9 wt% at a lower temperature between 75°C and 275°C. Chen *et al.* added a small amount of HMPA (hexamethylphosphoramide) to $LiAlH_4/LiNH_2$ mixture. 8.1 wt% H_2 can be released from the system at the ambient temperature, which is 370°C lower than the corresponding solid state dehydrogenation [81].

Transition metals (Ti, Cr, Fe, or Ni) were used to substitute for one Li sites in $LiNH_2$ and the interaction was calculated using first principles [82]. The electronic structures, N–H chemical bonds, and thermodynamics of these systems were calculated and analyzed. The Li–Ti–N–H system had a significant improvement in thermodynamics and a reaction enthalpy of –46.6 kJ· mol^{-1} is obtained while it is –75.67 $kJ{\cdot}mol^{-1}$ in the Li–N–H system.

3 Ammonia borane

NH_3BH_3 (AB in short) has been a subject of intensive study since 2000 [83] because of its potential to store a significant percent of hydrogen chemically (19.6 wt% H_2) and low molecular weight (30.7 $g{\cdot}mol^{-1}$). However, its stepwise dehydrogenation encounters relatively high kinetic barriers, which render temperatures higher than 100°C [83, 84]. Other drawbacks of ammonia borane for hydrogen storage include the irreversibility, emission of poisonous side products and severe material foaming in the dehydrogenation. Efficient methods are needed to dehydrogenate ammonia borane to release hydrogen at reasonable rates and moderate temperatures.

Metal catalyzed dehydrogenation, including metal-catalyzed solvolysis and metal-catalyzed thermolysis, is most widely studied among various methods for dehydrogenation of AB. So far, many metals and metal complexes have been found to catalyze ammonia borane solvolysis (Table 3). From these experimental results, we can find that the combination of higher dispersion with smaller particle sizes plays an important role in the active catalyst. While in metal-catalyzed thermolysis, Goldberg *et al.* reported the "fastest" thermolysis catalyst known for releasing 1 equiv. of hydrogen from ammonia borane by use of an iridium pincer complex, (POCOP)$Ir(H)_2$ (POCOP = [η^3–1, 3–(OP–tert–$Bu_2)_2C_6H_3$]) [85]. Chen *et al.* reported that Co and Ni nanoparticles doped ammonia borane samples evolved approximately 1 equiv. of hydrogen at a temperature as low as 59°C [86] (Fig. 1). In addition, many other

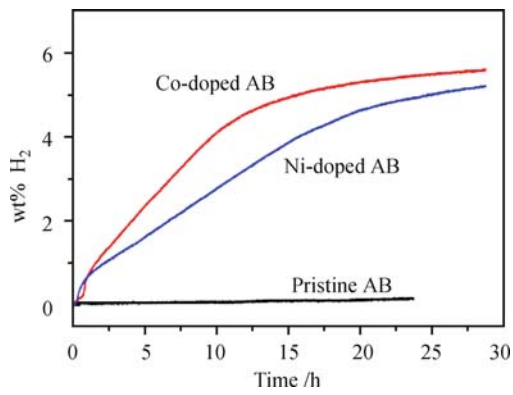

Fig. 1 The hydrogen capacities of Co and Ni nanoparticles doped AB comparing with pristine AB. Reproduced from Ref. [86], Copyright © 2009 American Chemistry Society.

Table 3 Different catalytic systems for solvolysis of ammonia borane.

Catalyst	Solvent	Eq. of H_2 released	Temp./°C	Time	Ref.
Pt (20% on C) (2 mol%)	H_2O	Approx 3	20	2 min	[88]
[Rh(1,5–cod)(μ–Cl)]$_2$ (2 mol%)		Approx 2.7		20 min	
Pd (2 mol%)		Approx 2.5		250 min	
Co (10% on C) (2 mol%)	H_2O	Approx 2.9	20	60 min	[89]
Ni (10% on γ–Al_2O_3) (2 mol%)		Approx 2.9		60 min	
Rh colloids (1 mol%)	H_2O	Approx 2.8	20	40 s	[90]
Ir colloids (1 mol%)		Approx 3		105 min	
Co colloids (1 mol%)		Approx 3		60 min	
$RuCl_3$ (0.5 mol%)	MeOH	Approx 3	20	5 min	[91]
Ni, Co, Cu nanoparticles	H_2O	Approx 3	20	20–300 min	[92]
$Ni_{0.88}Pt_{0.12}$ hollow sphere (2 mol%)	H_2O	Approx 3	20	30 min	[93]
Amorphous Fe nanoparticles	H_2O	Approx 3	20	8 min	[94]

metal complexes have also been investigated for AB analogues. That the metal catalysts Rh, Pd and Ru with a 0.5 mol% loading amount can dehydrogenate amine borane at room temperature has been reported by Manners [87].

Several other strategies for the dehydrogenation of AB have also been reported, such as acid-catalyzed dehydrogenation [95], ionic liquid catalyzed dehydrogenation [96] and metal amine activation [97], etc. Gutowska *et al.* reported the preparation of nanophase AB by incorporating AB into the channels of mesoporous silica SBA-15 [98]. The two notable effects resulting from the nanostructure of AB in SBA-15 scaffold include: 1) the temperature for H_2 release (m/e=2) being remarkably lower than that for neat AB, indicating an enhanced rate of H_2 release; and 2) the yield of the borazine (m/e=80) is significantly lower than that from neat AB. Recent study shows that AB filled in MOFs also enhances the dehydrogenation kinetics and eliminates the production of ammonia [99].

With the high potential driving force between the $H^{\delta+}$ in –NH_3 and $H^{\delta-}$ in metal hydrides, AB is readily deprotonated by a variety of metal hydrides to form a new family of metal amidoboranes. $LiNH_2BH_3$ and $NaNH_2BH_3$ were prepared by ball-milling solid AB with lithium or sodium hydride [100]. Li and Na amidoboranes released hydrogen at considerably lower temperatures than AB and at a dehydrogenation temperature of 90°C, 8 wt% and 6 wt% of hydrogen were released within the first hour without the unwanted by-product borazine. Burrell and co-workers synthesized $Ca(NH_2BH_3)_2$ by adding AB to CaH_2 in THF [97]. Whereas this compound releases hydrogen slowly at 90°C, only 0.3 equivalents of H_2 being released at this temperature. One more recent example is the synthesis of KNH_2BH_3 reported by Burrell *et al.* [101]. It is reported that KNH_2BH_3 evolves 6.5 wt% hydrogen at 80°C in several hours. At present, the main problem for these metal aminoboranes is the lack of facile reversibility.

4 Metal organic frameworks

Metal organic frameworks (MOFs) constructed from metal cation and cluster nodes linked by ligand linkers (as shown in Fig. 2) are an important class of new hybrid solids that show potential applications as storage materials for hydrogen, carbon dioxide and methane. Although physisorption of H_2 in porous hosts can be highly reversible via changes in pressure and/or temperature, the storage involves low binding energies and isosteric heats of adsorption and therefore cryogenic temperatures, typically 77 K, need to be used to achieve reasonable substrate uptake capacities.

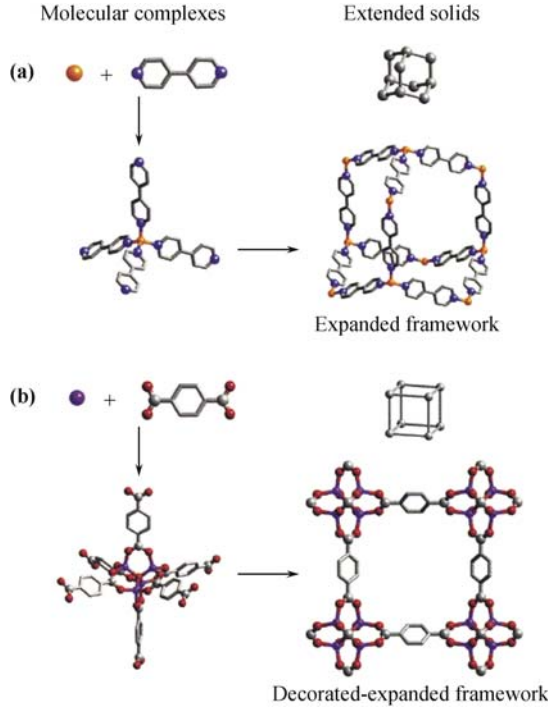

Fig. 2 The scheme of assembly of metal–organic frameworks. Reproduced from Ref. [102], Copyright © 2001 American Chemistry Society.

The isosteric heat of adsorption (Qst) of a MOFs–

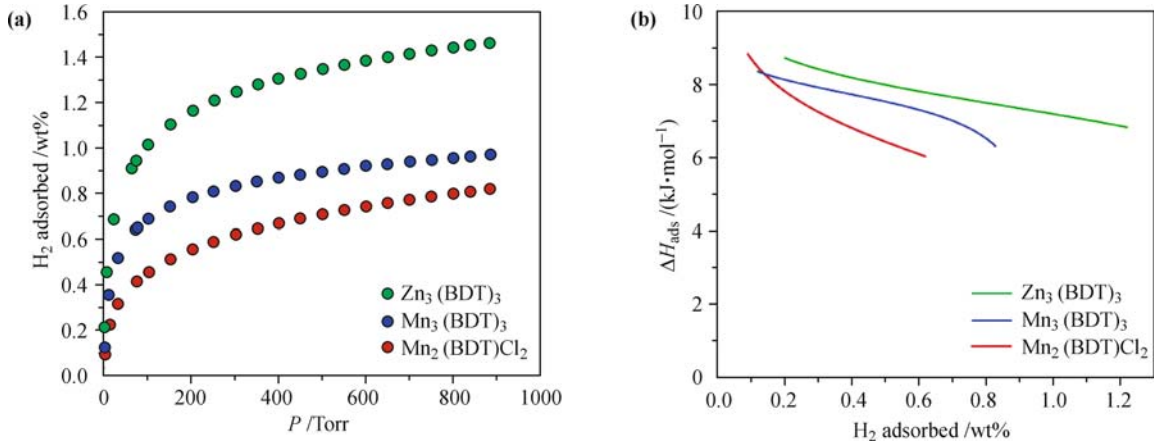

Fig. 3 **(a)** Adsorption isotherms for the H_2 uptake in desolvated samples at 77 K. **(b)** Enthalpy of adsorption plots as a function of the uptake of H_2 in desolvated samples. Reproduced from Ref. [106], Copyright © 2006 American Chemistry Society.

H_2 system is a key thermodynamic variable for hydrogen storage and gas separation [103]. The bottleneck of MOFs as hydrogen storage materials for vehicles is the low temperature owing to the weak isosteric heats of adsorption involved (typically 5–8 kJ·mol^{-1}) [104]. $[Mn(DMF)_6]_3[(Mn_4Cl)_3(BTT)_8(H_2O)_{12}]_2 \cdot 42DMF \cdot 11H_2O \cdot 20CH_3OH$ synthesized by Dinca has an adsorption heat of 10.1 kJ·mol^{-1}, which is the largest one among MOFs applied for hydrogen storage [105]. As shown in Fig. 3(a) and (b) [106], many researches demonstrated that H_2 uptake correlates with the heat of adsorption at low pressure [107].

Furthermore, it has been estimated that an adsorption heat of 15–30 kJ·mol^{-1} is required for MOFs materials with high hydrogen storage at room temperature within the pressure range 1.5–20 bar [104, 108, 109]. The isosteric heat of adsorption is a differential quantity usually determined with the Clausius–Clapeyron equation [110]:

$$Q_{st} = \frac{RT_1T_2\ln(P_2/P_1)}{T_2 - T_1} \quad (8)$$

The isosteric heat of adsorption at zero surface coverage is related to the energy of hydrogen adsorption and can be considered a measure of the extent of MOFs–H_2 interactions. The Qst values can be calculated using hydrogen-adsorption isotherms measured at different temperatures, otherwise, be simulated or calculated from Grand Canonical Monte Carlo simulations or density functional theory [108].

To enhance the heat of adsorption of H_2, many strategies were investigated, such as narrow pores, open metal centers and doping [111–121]. Using functional ligands to generate MOFs with narrow pores and increase the interaction energy of single H_2 molecule with the overlapping potential from opposite pore walls are considered to be effective [111]. Luo *et al.* provided structural evidence demonstrating for the first time that an optimal pore size (about 6–7 Å) enhances the interactions between H_2 molecules and pore walls. The pores with optimal size allow single H_2 molecule directly interact with the pore walls with stronger Vander Waals interaction, which is even stronger than the interaction between the H_2 molecule and the open metal site [112]. Yaghi *et al.* investigated IRMOFs synthesized from different organic linkers with similar net. They demonstrated that the organic linkers play important roles in defining pore sizes, providing organic adsorptive sites and altering the interaction of H_2 with the cluster due to differences in their electronic structures [113, 114].

Recently, MOFs with open metal centers have attracted great attention for their larger heats of adsorption (10 kJ·mol^{-1}) than classical MOFs (4–5 kJ·mol^{-1}) [115]. Yaghi and co-workers have already found that both the metal-oxide units and the organic linkers are important features for H_2 binding [113, 114, 116, 117]. Chen and co-workers showed that thermal removal of axial aqua ligands from MOF-505 exposed the unsaturated copper binding sites with a favorable impact on the hydrogen storage capacity [118]. Understanding the relation between the enhanced H_2 binding energy and the open metal sites is important for further research with an aim to improve the hydrogen storage capacity [119].

Beyond, doping with metal ions (Li) has been applied to increasing the binding energy of H_2 to MOFs [120, 121]. The $[H_2PPZ]^{2+}$ cation in the framework of $H_2PPZ[In(QPTC)]$ was found to act as a kinetic trap to give hysteresis in hydrogen uptake. Li^+ exchange eliminates the hysteresis in hydrogen adsorption completely. Analysis of the adsorption kinetics at various temperatures revealed that the energy barrier for hydrogen diffusion through the small windows is 15 kJ·mol^{-1} [122].

Among MOF-based materials, no material can satisfy the criteria delineated by the United States Department of Energy. To meet the criteria, large adsorption heat is

necessarily required.

5 Covalent organic frameworks

Apart from MOFs, the covalent organic frameworks (COFs) have been designed and successfully synthesized by Yaghi's group, which preserve the merits of good thermal stability, large surface area and extremely low mass density (0.17 $g \cdot cm^{-3}$ for COF-108). Therefore they are considered as additional prospective candidates for hydrogen storage [123–126]. Previous theoretical investigation predicts that the 3D COF-105 and COF-108 take in hydrogen over 10% at 298 K [127–129], Grand Canonical Monte Carlo simulations of hydrogen showed that the four 3D COFs materials might attain a 30% increase for the uptake compared with analogous simulations performed for metal organic frameworks at 77 K and 298 K [127]. Unfortunately, the hydrogen storage capacity at room temperature is still quite far from the DOE target of 6 wt%. The reason turns out to be the weak interaction between the hydrogen molecular and the materials (about 2∼5 $kJ \cdot mol^{-1}$) [128, 130, 131].

For practical hydrogen storage at the ambient condition (–30∼80°C and 1∼ 100 bars), the hydrogen adsorption energies between 9.6 $kJ \cdot mol^{-1}$ to 58 $kJ \cdot mol^{-1}$ was suggested [114]. To enhance the hydrogen adsorption energy, some prospective strategies of modifying the COFs materials have been proposed by first principle calculation. One possible way to improve the hydrogen adsorption energy is to simply mix additional metal atoms or ions into the materials [132]. The hydrogen adsorption energies were dramatically increased in Li and Mg ion-decorated COFs, and their saturated hydrogen storage capacities exceed the DOE target. Another way is to use the method of metal functionalization [133]. The calculation predicts that the insertion of lithium alkoxide groups into the COFs leads to the enhancement of the interaction between the H_2 and the materials (7.1 $kJ \cdot mol^{-1}$ per H_2) when five H_2 moleculars are being adsorbed. In addition, it is suggested that the metal atoms and B atom be incorporated with the COFs via the replacement of the non-metal atoms [134, 135], which will have improved the hydrogen adsorption energies and increased the hydrogen uptake at room temperature. However, those methods mentioned above do not have advantages in the practical application until now.

Recently, some new COFs materials have been designed with better hydrogen storage properties. Based on the COF-102, the phenylene moieties of COF-102 is substituted by other extended aromatic moieties without changing the net topology. These new COFs materials present superior hydrogen storage properties than the original COF-102. The Grand Canonical Monte Carlo simulation demonstrated that the hydrogen uptake gets as high as 6 wt% at room temperature [136]. Although these new designed COFs materials have not been synthesized in experimental, another modification on the COFs material (composed of phthalocyanine macrocycles joined by phenylene boronic acid linkers) has been implemented [137].

6 Zeolitic imidazolate frameworks

Zeolitic imidazolate frameworks (ZIFs), a new category of metal organic frameworks based on zeolitic topologies, are synthesized from reactions of transition-metal ions and imidazolate/imidazolate-type linkers. The bridging angles of imidazolate (IM) in <M–IM–M units is coincident with the Si–O–Si angle in zeolites and this has led to the use of imidazole and related ligands as tectons to form so-called ZIFs (Fig. 4). These materials possess more tunable structures as compared with traditional zeolites and appear to be promising materials for gas storage through adsorption because of their exceptional chemical and thermal stabilities [138–140].

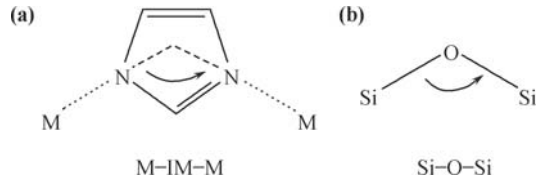

Fig. 4 The bridging angles in metal IMs **(a)** and zeolites **(b)**. Reproduced from Ref. [138], Copyright © 2006 National Academy of Sciences.

H_2 adsorption on ZIF-11 was reported to be 1.4 and 1.3 wt% for ZIF-8 at 1 bar and 77 K [139]. Yildirim *et al.* measured the adsorption of H_2 on ZIF-8 over large temperature and pressure ranges [141]. They also analyzed adsorption sites for D_2 molecules on ZIF-8 using neutron powder diffraction at low temperatures and found that the imidazolate linker is primarily responsible for adsorption. The total maximum gas uptake with these materials are not impressive compared to other more porous metal organic frameworks due to their relative low BET surface areas and pore volumes. However, the ZIF series provides a number of candidates for selective gas capture and adsorption.

7 Summary and outlook

Great efforts have been made to develop and understand solid-state reversible hydrogen storage materials. Although these materials show an encouraging progress, none of them qualify and fulfill all hydrogen storage criteria such as i) high hydrogen content (>6.0 wt%), ii) favorable or tuning thermodynamics (30–55 $kJ \cdot mol^{-1}$ H_2), iii) operate below 100°C for H_2 delivery, iv) onboard

refueling option for a hydrogen-based infrastructure, v) cyclic reversibility (about 1000 cycles) at moderate temperatures, and so on. Throughout all the hydrogen storage methods, thermodynamics and kinetics are the most important parameters for investigating the hydrogen uptake capacity. Nanosizing and nanoconfinement are now the new strategies towards meeting the requirement of higher hydrogen storage capacity for chemical storage systems such as metal hydrides and ammonia borane, etc. As for physical storage systems, it is really a challenge to find novel compounds with proper adsorption enthalpies. Theoretical calculation is worthy of deep study in order to understand the mechanism of various hydrogen storage materials, improve their thermodynamics and kinetics, and develop new materials with good performance. In conclusion, there are still challenging issues to be carefully addressed, including high storage capacity, suitable thermodynamics and fast kinetics.

Acknowledgements The authors gratefully acknowledged the financial support for this work from the National Basic Research Program of China (973 Program) (Grant No. 2010CB631303), the National Natural Science Foundation of China (Grant Nos. 20833009, 20873148, 20903095, 50901070, 51071146, 51071081, and U0734005), IUPAC (Project No. 2008-006-3-100), Dalian Science and Technology Foundation (Grant No. 2009A11GX052), Liaoning BaiQianWan Talents Program (Project No. 2010921050), and the State Key Laboratory of Explosion Science and Technology, Beijing Institute of Technology (Grant No. KFJJ10-1Z).

References

1. J. Graetz, Chem. Soc. Rev., 2009, 38(1): 73
2. S. Satyapal, J. Petrovic, C. Read, G. Thomas, and G. Ordaz, Catal. Today, 2007, 120(3–4): 246
3. P. Chen and M. Zhu, Mater. Today, 2008, 11(12): 36
4. L. Schlapbach and A. Züttel, Nature, 2001, 414(6861): 353
5. J. Yang, A. Sudik, C. Wolverton, and D. J. Siegel, Chem. Soc. Rev., 2010, 39(2): 656
6. B. Bogdanović and M. Schwickardi, J. Alloys Comp., 1997, 253–254(1–2): 1
7. J. A. Dilts and E. C. Ashby, Inorg. Chem., 1972, 11(6): 1230
8. S. S. Liu, L. X. Sun, Y. Zhang, F. Xu, J. Zhang, H. L. Chu, M. Q. Fan, T. Zhang, X. Y. Song, and J. P. Grolier, Int. J. Hydrogen Energy, 2009, 34(19): 8079
9. J. R. Ares, K. F. Aguey-Zinsou, M. Porcu, J. M. Sykes, M. Dornheim, T. Klassen, and R. Bormann, Mater. Res. Bull., 2008, 43(5): 1263
10. R. A. Varin and L. Zbroniec, J. Alloys Comp., 2010, 504(1): 89
11. A. Andreasen, T. Vegge, and A. S. Pedersen, J. Solid State Chem., 2005, 178(12): 3672
12. V. P. Balema, J. W. Wiench, K. W. Dennis, M. Pruski, and V. K. Pecharsky, J. Alloys Comp., 2001, 329(1–2): 108
13. J. Chen, N. Kuriyama, Q. Xu, H. T. Takeshita, and T. Sakai, J. Phys. Chem. B, 2001, 105(45): 11214
14. M. Resan, M. D. Hampton, J. K. Lomness, and D. K. Slattery, Int. J. Hydrogen Energy, 2005, 30(13–14): 1417
15. M. Resan, M. D. Hampton, J. K. Lomness, and D. K. Slattery, Int. J. Hydrogen Energy, 2005, 30(13–14): 1413
16. X. P. Zheng, X. H. Qu, I. S. Humail, P. Li, and G. Q. Wang, Int. J. Hydrogen Energy, 2007, 32(9): 1141
17. H. W. Brinks, A. Fossdal, J. E. Fonneløp, and B. C. Hauback, J. Alloys Comp., 2005, 397(1–2): 291
18. V. P. Balema, K. W. Dennis, and V. K. Pecharsky, Chem. Commun. (Camb.), 2000, (17): 1665
19. D. S. Easton, J. H. Schneibel, and S. A. Speakman, J. Alloys Comp., 2005, 398(1–2): 245
20. D. Blanchard, H. W. Brinks, B. C. Hauback, and P. Norby, Mater. Sci. Eng. B, 2004, 108(1–2): 54
21. J. R. Ares, K. F. Aguey-Zinsou, M. Elsaesser, X. Z. Ma, M. Dornheim, T. Klassen, and R. Bormann, Int. J. Hydrogen Energy, 2007, 32(8): 1033
22. Y. Suttisawat, P. Rangsunvigit, B. Kitiyanan, N. Muangsin, and S. Kulprathipanja, Int. J. Hydrogen Energy, 2007, 32 (9): 1277
23. T. Sun, C. K. Huang, H. Wang, L. X. Sun, and M. Zhu, Int. J. Hydrogen Energy, 2008, 33(21): 6216
24. L. H. Kumar, B. Viswanathan, and S. S. Murthy, Int. J. Hydrogen Energy, 2008, 33: 366
25. L. Zaluski, A. Zaluska, and J. O. Ström-Olsen, J. Alloy. Comp., 1999, 290(1–2): 71
26. F. H. Wang, Y. F. Liu, M. X. Gao, K. Luo, H. G. Pan, and Q. D. Wang, J. Phys. Chem. C, 2009, 113(18): 7978
27. A. W. Vittetoe, M. U. Niemann, S. S. Srinivasan, K. McGrath, A. Kumar, D. Y. Goswami, E. K. Stefanakos, and S. Thomas, Int. J. Hydrogen Energy, 2009, 34(5): 2333
28. S. S. Liu, L. X. Sun, J. Zhang, Y. Zhang, F. Xu, Y. H. Xing, F. Li, J. J. Zhao, Y. Du, W. Y. Hu, and H. Q. Deng, Int. J. Hydrogen Energy, 2010, 35(15): 8122
29. S. Sartori, A. Léon, O. Zabara, J. Muller, M. Fichtner, and B. C. Hauback, J. Alloys Comp., 2009, 476(1–2): 639
30. J. F. Mao, Z. P. Guo, H. K. Liu, and X. B. Yu, J. Alloy. Comp., 2009, 487(1–2): 434
31. J. F. Mao, X. B. Yu, Z. P. Guo, C. K. Poh, H. K. Liu, Z. Wu, and J. Ni, J. Phys. Chem. C, 2009, 113(24): 10813
32. J. Wang, A. D. Ebner, and J. A. Ritter, J. Am. Chem. Soc., 2006, 128(17): 5949
33. J. Graetz, J. Wegrzyn, and J. J. Reilly, J. Am. Chem. Soc., 2008, 130(52): 17790
34. X. F. Liu, G. S. McGrady, H. W. Langmi, and C. M. Jensen, J. Am. Chem. Soc., 2009, 131(14): 5032
35. S. Orimo, Y. Nakamori, G. Kitahara, K. Miwa, N. Ohba, S. Towata, and A. Züttel, J. Alloys Comp., 2005, 404–406: 427
36. Z. Z. Fang, P. Wang, T. E. Rufford, X. D. Kang, G. Q. Lu, and H. M. Cheng, Acta Mater., 2008, 56(20): 6257
37. N. Brun, R. Janot, C. Sanchez, H. Deleuze, C. Gervais, M. Morcrette, and R. Backov, Energy & Environ. Sci., 2010, 3: 824
38. A. F. Gross, J. J. Vajo, S. L. V. Atta, and G. L. Olson, J. Phys. Chem. C, 2008, 112(14): 5651
39. P. Ngene, P. Adelhelm, A. M. Beale, K. P. de Jong, and P. E. de Jongh, J. Phys. Chem. C, 2010, 114(13): 6163
40. F. W. Dafert and R. Miklauz, Monatsh. Chem., 1910, 31(9): 981
41. R. Juza and K. Opp, Z. Anorg. Allg. Chem., 1951, 266(6): 313
42. P. Chen, Z. T. Xiong, J. Z. Luo, J. Y. Lin, and K. L. Tan, Nature, 2002, 420(6913): 302
43. T. Ichikawa, N. Hanada, S. Isobe, H. Y. Leng, and H. Fujii, J. Phys. Chem. B, 2004, 108(23): 7887

44. P. Chen, Z. T. Xiong, J. Z. Luo, J. Y. Lin, and K. L. Tan, J. Phys. Chem. B, 2003, 107(39): 10967
45. T. Ichikawa, S. Isobe, N. Hanada, and H. Fujii, J. Alloys Comp., 2004, 365(1–2): 271
46. S. Isobe, T. Ichikawa, S. Hino, and H. Fujii, J. Phys. Chem. B, 2005, 109(31): 14855
47. T. Hao, M. Matsuo, Y. Nakamori, and S. Orimo, J. Alloys Comp., 2008, 458(1–2): L1
48. J. Z. Hu, J. H. Kwak, Z. G. Yang, W. Osborn, T. Markmaitree, and L. L. Shaw, J. Power Sources, 2008, 182(1): 278
49. H. Y. Leng, T. Ichikawa, S. Hino, and H. Fujii, J. Alloys Comp., 2008, 463(1–2): 462
50. S. D. Beattie, H. W. Langmi, and G. S. McGrady, Int. J. Hydrogen Energy, 2009, 34(1): 376
51. R. A. Varin, M. Jang, and M. Polanski, J. Alloys Comp., 2010, 491(1–2): 658
52. W. Osborn, T. Markmaitree, L. L. Shaw, J. Z. Hu, J. Kwak, and Z. G. Yang, Int. J. Hydrogen Energy, 2009, 34(10): 4331
53. W. Osborn, T. Markmaitree, L. L. Shaw, R. M. Ren, J. Z. Hu, J. H. Kwak, and Z. G. Yang, JOM, 2009, 61(4): 45
54. J. Z. Hu, J. H. Kwak, Z. Yang, W. Osborn, T. Markmaitree, and L. L. Shaw, J. Power Sources, 2008, 181(1): 116
55. W. Osborn, T. Markmaitree, and L. L. Shaw, Nanotechnology, 2009, 20(20): 204082
56. A. Blomqvist, C. M. Araujo, R. H. Scheicher, P. Srepusharawoot, W. Li, P. Chen, and R. Ahuja, Phys. Rev. B, 2010, 82(2): 024304
57. L. P. Ma, H. B. Dai, Z. Z. Fang, X. D. Kang, Y. Liang, P. J. Wang, P. Wang, and H. M. Cheng, J. Phys. Chem. C, 2009, 113(22): 9944
58. L. P. Ma, Z. Z. Fang, H. B. Dai, X. D. Kang, Y. Liang, P. J. Wang, P. Wang, and H. M. Cheng, J. Mater. Res., 2009, 24(6): 1936
59. H. Liu, Y. H. Zhang, and S. P. Huang, Chin. J. Chem. Phys., 2010, 23(1): 5
60. J. Lu, Y. J. Choi, Z. Z. Fang, and H. Y. Sohn, J. Power Sources, 2010, 195(7): 1992
61. T. Markmaitree and L. L. Shaw, J. Power Sources, 2010, 195(7): 1984
62. R. R. Shahi, T. P. Yadav, M. A. Shaz, and O. N. Srivastva, Int. J. Hydrogen Energy, 2010, 35(1): 238
63. M. Tsubota, S. Hino, H. Fujii, C. Oomatsu, M. Yamana, T. Ichikawa, and Y. Kojima, Int. J. Hydrogen Energy, 2010, 35(5): 2058
64. F. Dolci, E. Weidner, M. Hoelzel, T. Hansen, P. Moretto, C. Pistidda, M. Brunelli, M. Fichtner, and W. Lohstroh, Int. J. Hydrogen Energy, 2010, 35(11): 5448
65. Q. Wang, Y. G. Chen, C. L. Wu, M. D. Tao, and J. G. Gai, Chin. Sci. Bull., 2009, 54(3): 497
66. Q. Wang, Y. G. Chen, G. Niu, C. L. Wu, and M. D. Tao, Ind. Eng. Chem. Res., 2009, 48(11): 5250
67. J. C. Wang, H. L. Li, S. M. Wang, X. P. Liu, Y. Li, and L. J. Jiang, Int. J. Hydrogen Energy, 2009, 34(3): 1411
68. L. P. Ma, P. Wang, H. B. Dai, and H. M. Cheng, J. Alloys Comp., 2009, 468(1–2): L21
69. A. Sudik, J. Yang, D. Halliday, and C. Wolverton, J. Phys. Chem. C, 2008, 112(11): 4384
70. W. S. Tang, G. Wu, T. Liu, A. T. S. Wee, C. K. Yong, Z. T. Xiong, A. T. S. Hor, and P. Chen, Dalton Trans., 2008, 18(18): 2395
71. Y. X. Liu, S. Q. Yang, D. D. Zhang, G. X. Li, W. L. Wei, and J. Guo, J. Inorg. Mater., 2009, 24(4): 813
72. J. R. Hattrick-Simpers, J. E. Maslar, M. U. Niemann, C. Chiu, S. S. Srinivasan, E. K. Stefanakos, and L. A. Benderskyy, Int. J. Hydrogen Energy, 2010, 35(12): 6323
73. L. L. Li, B. Peng, Z. L. Tao, F. Y. Cheng, and J. Chen, Adv. Funct. Mater., 2010, 20(12): 1894
74. D. M. Liu, Q. Q. Liu, T. Z. Si, and Q. A. Zhang, J. Alloys Comp., 2010, 495(1): 272
75. A. Siangsai, Y. Suttisawat, P. Sridechprasat, P. Rangsunvigit, B. Kitiyanan, and S. Kulprathipanja, J. Chem. Eng. of Jpn, 2010, 43(1): 95
76. J. K. Yang, X. H. Wang, J. Mao, L. X. Chen, H. G. Pan, S. Q. Li, H. W. Ge, and C. P. Chen, J. Alloys Comp., 2010, 494(1–2): 58
77. A. Sudik, J. Yang, D. J. Siegel, C. Wolverton, R. O. Carter, and A. R. Drews, J. Phys. Chem. C, 2009, 113(5): 2004
78. M. U. Niemann, S. S. Srinivasan, A. Kumar, E. K. Stefanakos, D. Y. Goswami, and K. McGrath, Int. J. Hydrogen Energy, 2009, 34(19): 8086
79. K. Luo, Y. F. Liu, F. H. Wang, M. X. Gao, and H. G. Pan, Int. J. Hydrogen Energy, 2009, 34(19): 8101
80. M. U. D. Naik, S. U. Rather, C. S. So, S. W. Hwang, A. R. Kim, and K. S. Nahm, Int. J. Hydrogen Energy, 2009, 34(21): 8937
81. X. L. Zheng, W. L. Xu, Z. T. Xiong, Y. S. Chua, G. T. Wu, S. Qin, H. Chen, and P. Chen, J. Mater. Chem., 2009, 19(44): 8426
82. Q. A. Wang, Z. Q. Chen, W. B. Yu, Y. G. Chen, and Y. A. Li, Ind. Eng. Chem. Res., 2010, 49(13): 5993
83. G. Wolf, J. Baumann, F. Baitalow, and F. P. Hoffmann, Thermochim. Acta, 2000, 343(1–2): 19
84. M. G. Hu, R. A. Geanangel, and W. W. Wendlandt, Thermochim. Acta, 1978, 23(2): 249
85. M. C. Denney, V. Pons, T. J. Hebden, D. M. Heinekey, and K. I. Goldberg, J. Am. Chem. Soc., 2006, 128(37): 12048
86. T. He, Z. T. Xiong, G. T. Wu, H. L. Chu, C. Z. Wu, T. Zhang, and P. Chen, Chem. Mater., 2009, 21(11): 2315
87. C. A. Jaska, K. Temple, A. J. Lough, and I. Manners, J. Am. Chem. Soc., 2003, 125(31): 9424
88. M. Chandra and Q. Xu, J. Power Sources, 2006, 156(2): 190
89. Q. Xu and M. Chandra, J. Power Sources, 2006, 163(1): 364
90. T. J. Clark, G. R. Whittell, and I. Manners, Inorg. Chem., 2007, 46(18): 7522
91. P. V. Ramachandran and P. D. Gagare, Inorg. Chem., 2007, 46(19): 7810
92. S. B. Kalidindi, M. Indirani, and B. R. Jagirdar, Inorg. Chem., 2008, 47(16): 7424
93. F. Y. Cheng, H. Ma, Y. M. Li, and J. Chen, Inorg. Chem., 2007, 46(3): 788
94. J. M. Yan, X. B. Zhang, S. Han, H. Shioyama, and Q. Xu, Angew. Chem. Int. Ed., 2008, 47(12): 2287
95. F. H. Stephens, R. T. Baker, M. H. Matus, D. J. Grant, and D. A. Dixon, Angew. Chem. Int. Ed., 2007, 46(5): 746
96. M. E. Bluhm, M. G. Bradley, U. Butterick, Kusari, and L. G. Sneddon, J. Am. Chem. Soc., 2006, 128(24): 7748
97. H. V. K. Diyabalanage, R. P. Shrestha, T. A. Semelsberger, B. L. Scott, M. E. Bowden, B. L. Davis, and A. K. Burrell, Angew. Chem. Int. Ed., 2007, 46(47): 8995
98. A. Gutowska, L. Y. Li, Y. S. Shin, C. M. M. Wang, X. H. S. Li, J. C. Linehan, R. S. Smith, B. D. Kay, B. Schmid, W. Shaw, M. Gutowski, and T. Autrey, Angew. Chem. Int. Ed., 2005, 44(23): 3578

99. Z. Y. Li, G. S. Zhu, G. Q. Lu, S. L. Qiu, and X. D. Yao, J. Am. Chem. Soc., 2010, 132(5): 1490
100. Z. T. Xiong, C. K. Yong, G. T. Wu, P. Chen, W. Shaw, A. Karkamkar, T. Autrey, M. O. Jones, S. R. Johnson, P. P. Edwards, and W. I. F. David, Nat. Mater., 2008, 7(2): 138
101. H. V. K. Diyabalanage, T. Nakagawa, R. P. Shrestha, T. A. Semelsberger, B. L. Davis, B. L. Scott, A. K. Burrell, W. I. F. David, K. R. Ryan, M. O. Jones, and P. P. Edwards, J. Am. Chem. Soc., 2010, 34(34): 11836
102. M. Eddaoudi, D. B. Moler, H. Li, B. Chen, T. M. Reineke, M. O'Keeffe, O. M. Yaghi, Acc. Chem. Res., 2001, 34: 319.
103. S. Sircar, R. Mohr, C. Ristic, and M. B. Rao, J. Phys. Chem. B, 1999, 103: 6539
104. Y. Yan, I. Telepeni, S. H. Yang, X. Lin, W. Kockelmann, A. Dailly, A. J. Blake, W. Lewis, G. S. Walker, D. R. Allan, S. A. Barnett, N. R. Champness, and M. Schröder, J. Am. Chem. Soc., 2010, 132(12): 4092
105. M. Dincă A. Dailly, Y. Liu, C. M. Brown, D. A. Neumann, and J. R. Long, J. Am. Chem. Soc., 2006, 128(51): 16876
106. M. Dinca, A. F. Yu, and J. R. Long, J. Am. Chem. Soc., 2006, 128(27): 8904
107. H. Frost, T. Düren, and R. Q. Snurr, J. Phys. Chem. B, 2006, 110(19): 9565
108. K. Sillar, A. Hofmann, and J. Sauer, J. Am. Chem. Soc., 2009, 131(11): 4143
109. H. Furukawa, M. A. Miller, and O. M. Yaghi, J. Mater. Chem., 2007, 17(30): 3197
110. S. Y. Qi, K. J. Hay, M. J. Rood, and M. P. Cal, J. Environ. Eng., 2000, 126(3): 267
111. B. Assfour and G. Seifert, Int. J. Hydrogen Energy, 2009, 34(19): 8135
112. J. H. Luo, H. W. Xu, Y. Liu, Y. S. Zhao, L. L. Daemen, C. Brown, T. V. Timofeeva, S. Q. Ma, and H. C. Zhou, J. Am. Chem. Soc., 2008, 130(30): 9626
113. J. L. Rowsell, J. Eckert, and O. M. Yaghi, J. Am. Chem. Soc., 2005, 127(42): 14904
114. A. G. Wong-Foy, A. J. Matzger, and O. M. Yaghi, J. Am. Chem. Soc., 2006, 128(11): 3494
115. W. Zhou and T. Yildirim, J. Phys. Chem. C, 2008, 112(22): 8132
116. N. L. Rosi, J. Eckert, M. Eddaoudi, D. T. Vodak, J. Kim, M. O'Keeffe, and O. M. Yaghi, Science, 2003, 300(5622): 1127
117. J. L. Rowsell, A. R. Millward, K. S. Park, and O. M. Yaghi, J. Am. Chem. Soc., 2004, 126(18): 5666
118. B. Chen, N. Ockwig, A. Millward, D. Contreras, and O. Yaghi, Angew. Chem. Int. Ed., 2005, 117(30): 4823
119. Q. Yang and C. Zhong, J. Phys. Chem. B, 2006, 110(2): 655
120. N. S. Venkataramanan, R. Sahara, H. Mizuseki, and Y. Kawazoe, Int. J. Mol. Sci., 2009, 10(4): 1601
121. K. L. Mulfort, T. M. Wilson, M. R. Wasielewski, and J. T. Hupp, Langmuir, 2009, 25(1): 503
122. S. Yang, X. Lin, A. J. Blake, G. S. Walker, P. Hubberstey, N. R. Champness, and M. Schroder, Nat. Chem., 2009, 1(6): 487
123. A. P. Côté, A. I. Benin, N. W. Ockwig, M. O'Keeffe, A. J. Matzger, and O. M. Yaghi, Science, 2005, 310(5751): 1166
124. H. M. El-Kaderi, J. R. Hunt, J. L. Mendoza-Cortés, A. P. Côté, R. E. Taylor, M. O'Keeffe, and O. M. Yaghi, Science, 2007, 316(5822): 268
125. A. P. Côté, H. M. El-Kaderi, H. Furukawa, J. R. Hunt, and O. M. Yaghi, J. Am. Chem. Soc., 2007, 129(43): 12914
126. J. R. Hunt, C. J. Doonan, J. D. LeVangie, A. P. Côté, and O. M. Yaghi, J. Am. Chem. Soc., 2008, 130(36): 11872
127. G. Garberoglio, Langmuir, 2007, 23(24): 12155
128. S. S. Han, H. Furukawa, O. M. Yaghi, and Goddard, J. Am. Chem. Soc., 2008, 130(35): 11580
129. E. Tylianakis, E. Klontzas, and G. E. Froudakis, Nanotechnology, 2009, 20(20): 204030
130. E. Klontzas, E. Tylianakis, and G. E. Froudakis, J. Phys. Chem. C, 2008, 112(24): 9095
131. H. Furukawa and O. M. Yaghi, J. Am. Chem. Soc., 2009, 131(25): 8875
132. Y. J. Choi, J. W. Lee, J. H. Choi, and J. K. Kang, Appl. Phys. Lett., 2008, 92(17): 173102
133. E. Klontzas, E. Tylianakis, and G. E. Froudakis, J. Phys. Chem. C, 2009, 113(50): 21253
134. F. Li, J. J. Zhao, B. Johansson, and L. X. Sun, Int. J. Hydrogen Energy, 2010, 35(1): 266
135. X. L. Zou, G. Zhou, W. H. Duan, K. Choi, and J. Ihm, J. Phys. Chem. C, 2010, 114(31): 13402
136. E. Klontzas, E. Tylianakis, and G. E. Froudakis, Nano Lett., 2010, 10(2): 452
137. E. L. Spitler and W. R. Dichtel, Nat. Chem., 2010, 2(8): 672
138. K. S. Park, Z. Ni, A. P. Côté, J. Y. Choi, R. D. Huang, F. J. Uribe-Romo, H. K. Chae, M. O'Keeffe, and O. M. Yaghi, Proc. Natl. Acad. Sci. USA, 2006, 103(27): 10186
139. H. Hayashi, A. P. Côté, H. Furukawa, M. O'Keeffe, and O. M. Yaghi, Nat. Mater., 2007, 6(7): 501
140. A. Phan, C. J. Doonan, F. J. Uribe-Romo, C. B. Knobler, M. O'Keeffe, and O. M. Yaghi, Acc. Chem. Res., 2010, 43(1): 58
141. H. Wu, W. Zhou, and T. Yildirim, J. Am. Chem. Soc., 2007, 129(17): 5314